Received: 29 August 2022 | Accepted: 8 April 2023

DOI: 10.1111/1365-2435.14348

Functional Ecology | BRITISH ECOLOGICAL SOCIETY

RESEARCH ARTICLE

Drought susceptibility of southern African C_4 grasses: Phylogenetically and photosynthetically determined?

Sarah L. Raubenheimer[1,2] | Nic Venter[3] | Brad S. Ripley[1]

[1]Department of Botany, Rhodes University, Grahamstown, South Africa

[2]Institute for Global Change Biology, School for Environment and Sustainability, University of Michigan, Ann Arbor, Michigan, USA

[3]School of Animal, Plant and Environmental Sciences, University of the Witwatersrand, Johannesburg, South Africa

Correspondence
Sarah L. Raubenheimer
Email: sarah.l.raubenheimer@gmail.com

Funding information
Rhodes University Research Council

Handling Editor: Guillaume Chomicki

Abstract

1. Factors that determine C_4 grass distributions have been well documented, with evidence in the literature for C_4 photosynthetic subtypes displaying varying levels of drought susceptibility. However, the interactions between C_4 photosynthetic subtype and phylogeny add complexity and are relatively under studied.
2. We use species distribution modelling to determine the influence of rainfall on distribution patterns of representative C_4 grass families and subtypes. Select C_4 grass species, representing different photosynthetic subtypes (NADP-Me and NAD-Me) and lineages (Panicoideae and Aristidoideae), were subjected to a progressive 58-day drought period and recovery phase, to explore drought responses through leaf water relations, gas exchange and chlorophyll fluorescence.
3. We show Panicoideae NADP-Me species to be more susceptible to drought than both Panicoideae NAD-Me and Aristidoideae NADP-Me species due to apparent greater metabolic impairment. The differences between groups were related to how rapidly photosynthesis declines with exposure to drought and the rate of recovery post-drought, rather than the maximum extent of photosynthetic decline. The mechanisms for the relative maintenance of plant water status differed between the Panicoideae NAD-Me species, which utilized greater stomatal control, and the Aristidoideae NADP-Me species, which maintained water uptake through osmotic adjustment.
4. *Synthesis*. We show here that drought susceptibility differs both phylogenetically and according to photosynthetic subtype, but that the role of phylogeny may outweigh physiological control. This research adds novel insight into the physiological differences behind observed rainfall-related differences in C_4 grass distribution patterns.

KEYWORDS
C_4 grasses, C_4 photosynthesis, drought susceptibility, NAD-Me, NADP-Me, southern Africa

1 | INTRODUCTION

C_4 grasses dominate much of the warm-climate grassland and savanna biomes globally. These ecosystems are particularly susceptible to climate change as their life histories are short and allow for rapid species composition changes (Smith & Donoghue, 2008). The predicted increases in aridity throughout southern Africa (Engelbrecht et al., 2015) necessitate a firm understanding of the drought responses of grassland species. Although the selective pressures that prompted the evolution of the C_4 pathway are reasonably

[Correction added on 17 May 2023, after first online publication: The affiliation of Brad S. Ripley has been corrected].

well studied (Sage, 2004) the relationship between different C_4 carboxylation subtypes and phylogenetic groups in determining drought tolerance is not fully understood (Edwards & Still, 2008; Furbank, 2011). This study aims to compare the mechanisms associated with drought tolerance between some of these functional groups and to discover how differences in tolerance correlate with species distributions.

Factors that determine C_4 grass distributions have been well documented, but the interactions between C_4 photosynthetic subtype and phylogeny (Sage & Monson, 1998) add complexity, particularly in responses to rainfall gradients (Carmo-Silva et al., 2009). The intrinsic differences between the three C_4 biochemical pathways (i.e. subtypes—NADP-Me, NAD-Me and PCK) show flexibility which could be developmentally and environmentally controlled (Furbank, 2011). This suggests that photosynthetic subtype could confer advantages under different conditions (Taub, 2000; Tieszen et al., 1979; Visser et al., 2012). Empirical data suggest that the abundance of C_4 grass species of the NADP-Me subtype increases with precipitation while that of NAD-Me species shows the reciprocal response (Cabido et al., 2008; Ellis et al., 1980; Taub, 2000; Vogel et al., 1986). However, this trend is complicated by phylogenetic interaction. For example, in South Africa, distributions indicate that Panicoideae species (mainly NADP-Me but also NAD-Me species) occur in more mesic habitats, while Aristidoideae species (also NADP-Me) occur in more arid environments (Visser et al., 2012).

Species distributions (Taub, 2000; Visser et al., 2012) demonstrate that Panicoideae NAD-Me species display higher physiological drought tolerance than Panicoideae NADP-Me species (Cabido et al., 2008; Hattersley & Watson, 1992). NAD-Me species exhibit greater leaf-level water-use efficiency (WUE) and drought tolerance than NADP-Me species, enabling greater conservation of plant water status (Ghannoum et al., 2002; Liu & Osborne, 2015; Wigley-Coetsee & Staver, 2020). However, the C_4 Aristidoideae, all of which are NADP-Me species, are generally limited to more arid regions, suggesting that they are more tolerant of drought than either panicoid photosynthetic subtype (Visser et al., 2012). This suggests that it may be phylogenetic group rather than photosynthetic subtype that determines drought tolerance and habitat preference (Cabido et al., 2008; Vogel et al., 1986). The interactions between C_4 subtype and lineage have been studied to some extent (Liu & Osborne, 2015; Pinto et al., 2016). However, to our knowledge, no studies have yet examined the responses of Aristidoideae species to drought and the mechanisms for the group's apparent drought tolerance (based on distribution patterns) remain to be elucidated. This, as well as a relative lack of Aristidoideae drought responses in the literature, presents a novel gap in the literature on C_4 grass responses to water limitations.

This study aims to examine the physiological mechanisms underpinning global patterns of differences in distributions between Panicoideae NADP-Me, Panicoideae NAD-Me and Aristidoideae NADP-Me groups using southern African representatives to determine physiological differences in drought tolerance. Our comparison is between plants with different photosynthetic subtypes (NADP-Me and NAD-Me) from the same lineage (Panicoideae) and between plants with the same subtype (NADP-Me), but from different lineages (Panicoideae and Aristidoideae). We use (a) species distribution modelling to confirm expectations of subtype and lineage distributions in relation to rainfall; and (b) experimental drought manipulation, where plants were subjected to a progressive 58-day drought period and a recovery phase, to explore drought responses through leaf water relations, gas exchange and chlorophyll fluorescence. We hypothesize that (1) Panicoideae NAD-Me species will show a greater tolerance of progressive drought and recovery from drought than Panicoideae NADP-Me species; and (2) Aristidoideae NADP-Me species will show a greater tolerance of progressive drought and recovery from drought than both groups of Panicoideae species despite the NADP-Me pathway being associated with lower drought tolerance. These hypotheses are based on the species occurrence, associated climate (Cabido et al., 2008; Ellis et al., 1980; Taub, 2000; Vogel et al., 1986) and physiological (Ghannoum et al., 2002; Liu & Osborne, 2015) patterns reported in the literature. Although we do not directly assess future scenarios, such phylogenetic and photosynthetic subtype interactions could help explain distribution patterns and provide valuable information for predictions of grassland distribution and functional composition under future climate scenarios.

2 | MATERIALS AND METHODS

2.1 | Species distribution modelling

Maximum entropy models (MaxEnt) species distribution models (SDMs) were developed using the maximum entropy algorithm implemented in MaxEnt v.3.3.3k to display the current SDMs for an array of C_4 grass species from the Panicoideae and Aristidoideae families. MaxEnt use machine-learning principles to predict the presence/absence of species across geographic space based on the relationship between site-specific environmental conditions and species occurrence records (Elith et al., 2011). From this, MaxEnt models can predict a measure of habitat suitability (H.S.) for a particular species in a particular location. H.S. is a factor of both the density of individuals of a species and the likelihood of the species being present (Elith et al., 2011). Although there are limitations to the chosen method (e.g. using solely presence data as opposed to presence–absence records; Phillips et al., 2009), MaxEnt SDMs provide a good base from which to guide our physiological hypotheses. SDMs were run for the study species as well as for multiple southern African Panicoideae and Aristidoideae species to confirm that patterns held throughout the groups (see species listed in Table S1). Models were separated into (a) 'study species models' which includes three species of Panicoideae NADP-Me, two species of Panicoideae NAD-Me and three species of Aristidoideae NADP-Me and (b) 'multi-species models' which includes multiple Panicoideae (38 species) and Aristiodoideae (6 species) species that occur in southern Africa. Species occurrence records were obtained from the Global Biodiversity Information Facility (https://www.gbif.org; Gbif.org, 2021) accessed on 20 November 2021. Environmental spatial data

were obtained from the WorldClim—Global Climate Data database (http://www.worldclim.org; Fick & Hijmans, 2017), providing 19 environmental layers for MaxEnt modelling (see Table S2). MaxEnt models were trained with the whole extent of southern Africa as the species maximum potential ranges. The MaxEnt models produced a spatial 'H.S.' based on a scale from 0 to 1 for southern Africa (including South Africa, Lesotho, eSwatini, Botswana, Namibia, Zimbabwe, Mozambique, Angola, Zambia, Malawi, Tanzania and the Democratic Republic of Congo) as well as probability curves relating to each environmental variable. Of most interest for this study was the correlation between precipitation and H.S., comparing areas of peak occurrence along a rainfall gradient between plant groups. Area under the curve (AUC) values were used to assess model performance using 10,000 random pseudoabsences during model evaluation. AUC values for all models were >0.85, and mean AUC was 0.94 (Table S1).

2.2 | Plant collection, growth conditions and experimental set-up

The species classified as 'study species' in the models were experimentally grown and studied in a drought manipulation experiment (see Table S3 for more detailed information of each species). *Tristachya leucothrix*, *Heteropogon contortus*, *Aristida diffusa* and *Aristida congesta* were collected from the Makhanda area (previously Grahamstown, Eastern Cape, South Africa), while *Aristida junciformis* was collected at Port Alfred (Eastern Cape, South Africa). Whole plants were dug up in the field, trimmed and potted such that each pot represented an individual plant. *Panicum coloratum*, *P. stapfianum* and *Alloteropsis semialata* were grown from existing potted plants that were trimmed and repotted. *Alloteropsis semialata* was collected at Middelburg, Gauteng Province, South Africa, (S25°50′, E29°24′), and *P. coloratum* was grown from seed sourced by Taylor et al. (2010). All plants were potted in 10 L pots containing 6.7 kg of a homogenous soil mixture made from locally obtained top-soil, representative of the soil the grasses grow in naturally, and kept in a clear polythene tunnel at the Department of Botany, Rhodes University. Average min/max temperatures (±SD) of the tunnel for the duration of the experiment were 17.6 ± 1.2 and 34.1 ± 4.6°C respectively and the average tunnel temperature was 25.1 ± 8.8°C. Diurnal photosynthetically active radiation (PAR) in the tunnel ranged from 64 to 1014 μmol s^{-1} m^{-2}, with midday values of 1012 ± 2 μmol s^{-1} m^{-2}. Plants were well watered (using field capacity of the soil as a guide) and hydroponic fertilizer (Chemicult—1 g L^{-1}) was added twice in the month leading up to the experiments. Six treatment and six control replicates (except *P. coloratum* and *A. diffusa* which had five replicates due to mortality) of each species were used in all the experiments.

Progressive drought was imposed by starting experiments with potted plants watered to field capacity (±20% soil water content [SWC]), and then allowing them to decrease SWC by ±0.3% each day over the subsequent 58 days (see Figure 1). This daily reduction is representative of natural soil drying (Ripley et al., 2010). On day 58, plants were rewatered and maintained at field capacity over the remaining 11 days (recovery phase). During the dry-down phase of the experiment, potted plants were weighed every second day, and supplementary water added where necessary to ensure that all plants dehydrated at similar rates. Field capacity of the soil was determined by soaking pots in water for 24 h and then allowing the soil to drain to constant mass under gravity. During this period, the evaporation from the soil surface was minimized by covering the pots with plastic lids. To estimate SWC it was necessary to determine the dry weight of the soil added to each pot and to estimate the weight of the plants. Soil dry weights were determined by oven-drying soil at 70°C for 72 h and representative plant weights were determined by harvesting a subset of plants from each species. Evaporation from the soil during the experiment was minimized by adding 1 kg of fine stone (<1 cm diameter) to the soil surface. Hence as plant, soil, pot and stone weights were accounted for, the % SWC for the potted plants could be calculated as $\text{SWC}(\%) = \frac{\text{soil wet mass} - \text{soil dry mass}}{\text{soil dry mass}} \times 100$.

2.3 | Leaf gas exchange, chlorophyll fluorescence and plant water relations

Gas exchange, chlorophyll fluorescence and leaf water relations (Leaf Ψ and RLWC) were measured on various occasions during the dehydration and rewatering phase of the experiment (Figure 1). Instantaneous measures of net CO_2 assimilation rates (A), stomatal conductance (G_{st}), intrinsic water-use efficiency (A/G_{st}) and intercellular CO_2 concentration (C_i) were conducted on the youngest fully expanded leaf (first down from the apical bud) of the control and treatment plants. These parameters were measured on the days indicated in Figure 1, except for the Aristidoideae species which were not measured on day 10. Measurements were made using a Li-6400-40 LCF photosynthesis system (Li-Cor Inc.) between 10:30 AM and 3:30 PM under laboratory conditions. Plants were acclimated under a sodium vapour light at a photosynthetic photon flux density (PPFD) similar to that used in the leaf chamber. Cuvette conditions were maintained as follows: incoming (reference) ambient CO_2 concentration (C_a) was supplied at 400 μmol mol^{-1}, a PPFD of 1200 μmol m^{-2} s^{-1} was supplied by a blue-red LED light source, leaf temperature was set at 29°C and vapour pressure deficits (VPDs) ranged between 1 and 2.5 kPa. Leaf areas were measured and entered manually, and gas exchange parameters were calculated according to the equations of Von Caemmerer and Farquhar (1981). To ensure that measurements were conducted at near saturating light intensities, photosynthetic response to incident light intensity was measured on control plants according to Long and Bernacchi (2003).

Chlorophyll fluorescence measurements were made immediately following each gas exchange measurement as not to disrupt the steady-state photosynthesis. Leaves were acclimated until steady-state fluorescence (F_s) was achieved. A multiphase flash (MPF) protocol was used to ensure maximum reduction of QA. The following MPF settings were used: 30% ramp, 250 ms for phase 1 and 3 and 500 ms for phase 2. The light intensity required to ensure

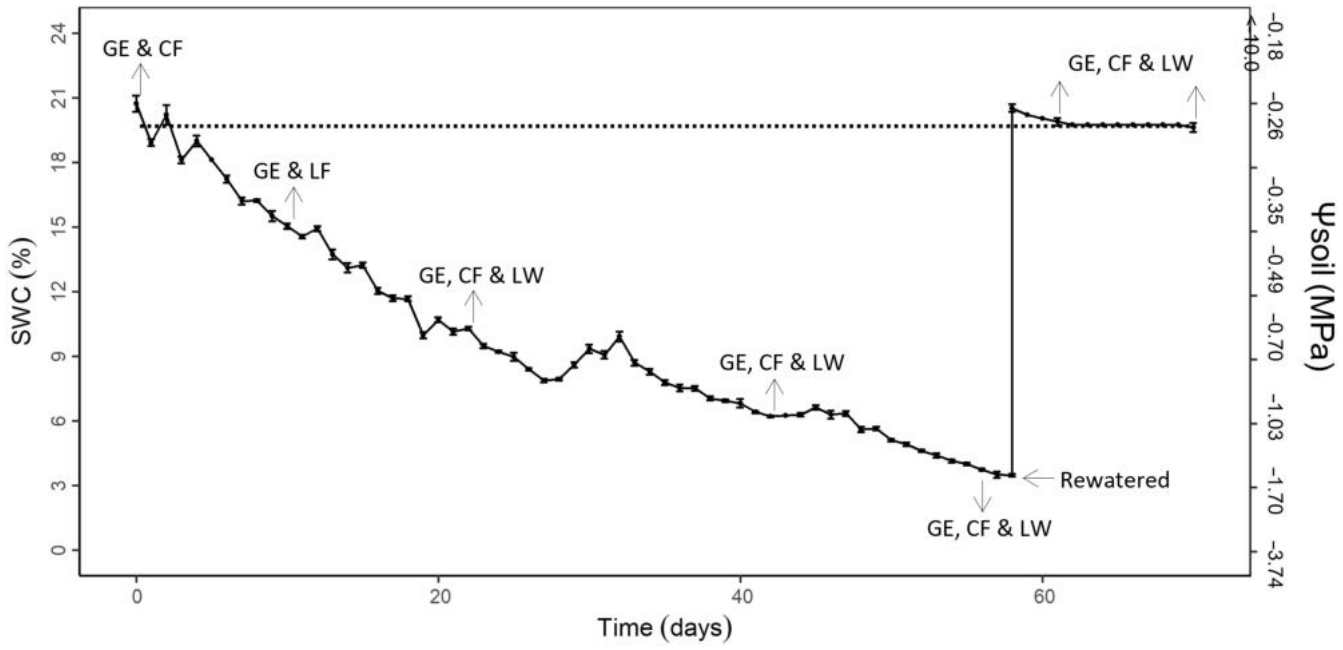

FIGURE 1 Soil water content (SWC) and corresponding soil water potential (Soil Ψ) for treatment (𝔱) and control plants (····) during the pot dry-down and rewatering phases of the experiment averaged across all nine species and replicates ($n = 106$). The occasions on which experimental measurements were conducted are superimposed: CF, chlorophyll fluorescence; GE, gas exchange; LW, leaf water relations (Leaf Ψ and RLWC). Control measurements (not shown) were performed on the same days those treatments were measured, except for Aristidoideae species where gas exchange and leaf water relations measurements were not done on days 10 and 70 due to time and weather constraints. For all plants, day 61 control data were used as the control for days 56 and 61 treatments.

QA reduction was experimentally determined. Chlorophyll fluorescence parameters measured are defined (Baker, 2008) and where necessary their calculations and units are shown. PSII maximum efficiency, $Fv'/Fm' = (Fm' - Fo')/Fm'$. At a given PPFD, this estimates the maximum PSII photochemistry (efficiency of oxidized [QA] PSII reaction centres). Fm' is the maximal fluorescence during the saturating light phase ($PPFD > 7000\,\mu mol\,m^{-2}\,s^{-1}$) (QA maximally reduced) and Fo' is the minimal fluorescence of a briefly darkened (6 s at 740 nm), light-adapted leaf (QA maximally oxidized). PSII operating efficiency, $\Phi PSII = (Fm' - Fs)/Fm'$. At a given PPFD, this estimates the efficiency at which light absorbed by PSII is used for QA reduction, (steady-state photosynthesis). Photochemical quenching, $qP = (Fm' - Fs)/(Fm' - Fo')$. At a given PPFD, this estimates the PSII reaction centres (QA) that are oxidized. This includes photosynthesis and photorespiration. Electron transport rate, $ETR = \Phi PSII \times f \times I \times \alpha leaf$ (μmol electrons $m^{-2}\,s^{-1}$), where $f = 0.5$ and $\alpha leaf = 0.85$.

2.4 | Midday leaf water potentials, relative leaf water contents and osmotic adjustment

The leaves used for gas exchange measurements were either excised at midday on the same day as the gas exchange measurements or on the following day. The excised leaves were immediately weighed, and the leaf water potential (Leaf Ψ) was measured using a Schőlander pressure chamber. Following Leaf Ψ measurements, the leaves were placed upright in a glass vial which contained enough water to cover the first 10 mm of the excised end of the leaf. The leaves were left in the dark overnight to regain full turgor pressure. The following morning the leaves were blotted, weighed and then placed in a drier at 70°C for 48 h, after which they were weighed again. This method allowed the Leaf Ψ and relative leaf water content (RLWC) to be obtained for the same leaf. Trial experiments were conducted to determine if the measurement of Leaf Ψ with a pressure chamber affected the rehydration of leaves and it was found to have no significant effect. $RLWC = \frac{\text{leaf wet mass} - \text{leaf dry mass}}{\text{leaf turgid mass} - \text{leaf dry mass}} \times 100$. Leaf Ψ could not accurately be measured at day 56 (±3.5% SWC) because of the extreme leaf dehydration. Ghannoum et al. (2003) showed that the relationship of Leaf Ψ to RLWC was mostly linear. Models were fitted to the mean Leaf Ψ and corresponding RLWC data for each species (control and treatment plants) during the drought and recovery phase. All the species showed a linear relationship of Leaf Ψ to RLWC, thus a straight-line function ($y = mx - c$) was used to describe Leaf Ψ at day 56 (see Figure S3).

Pressure volume (PV) curves were constructed by determining the relationship between RLWC and Leaf Ψ (see Figure S3). This was done by sequentially dehydrating leaves and determining Leaf Ψ and RLWC at regular intervals. Initially well-watered potted rooted plants were bagged overnight to ensure the leaves reached full turgor potential. For 11 replicate plants, the fully expanded second or third leaf produced after the cotyledon was excised, weighed and the corresponding Leaf Ψ was obtained by using the Schőlander pressure chamber. Subsequent leaves were allowed to slowly dehydrate in a humidified bell jar and Leaf Ψ and RLWC were measured at repeated intervals. PV curves constructed from control leaves were

used to determine individual components of leaf water potential (Leaf $\Psi = \Psi P + \Psi\pi$; see Figure S4). The reciprocal of the Leaf Ψ was plotted against RLWC and a model was fitted to the data using the equations of Schulte and Hinckley (1985). The TLP ($\Psi P = 0$ MPa) was defined as the RLWC at which Leaf Ψ equalled $\Psi\pi$ (osmotic potential). $\Psi\pi$ at 100% RLWC was calculated as the y-intercept of the straight line. To determine the osmotic adjustment (OA) of treated plants, their Leaf Ψ and RLWC were measured at various intervals during the dry-down experiment, once RLWC had declined sufficiently to ensure that $\Psi P = 0$ and that changes in 1/Leaf Ψ were solely dependent on $1/\Psi\pi$. This response of 1/Leaf Ψ to RLWC was fitted with a straight line and $1/\Psi\pi$ at 100% RLWC (*y*-intercept) was calculated. OA was calculated from the change in $\Psi\pi$ with drought stress. This was expressed in absolute terms for well-watered individuals or relative to the values for well-watered controls for individuals exposed to drought. Osmotic adjustment was defined as the difference between $\Psi\pi$ of control and drought-treated plants at 100% RLWC. As different species showed inherently different $\Psi\pi$, OA was expressed as a percentage of the control value (relative OA) to allow the comparison of OA between species.

2.5 | Statistics

The data obtained were analysed using the R language and platform (R Core Team, 2020). To determine the influence of the treatments (both plant type and days of exposure to drought) on plant ecophysiology and water relations, linear mixed-effects models were fitted in R using the 'nlme' package (Pinheiro et al., 2007). Species were treated as a random factor in the models. The use of planting treatment as a random factor in the statistical models was initially included to avoid planting differences between species influencing the results but was removed once it was determined that it had no effect on the statistical results. ANOVAs were conducted on the mixed-effect model outputs to get appropriate pairwise and global model statistics. Statistics presented in the results show the interaction between plant type and days of exposure to drought (i.e. differences between plant types in responses to drought over time). Comparisons including watered (control) plants are presented in Figure S2. Model evaluation was conducted for all MaxEnt models run, ensuring the Average AUC values were greater than 0.7. To determine the difference in H.S. relative to mean annual precipitation between plant types, χ^2 tests were conducted on generalized additive model (GAM) distributions using the 'gam' package in R (Hastie, 2020).

3 | RESULTS

3.1 | Species distributions in relation to rainfall

Maximum entropy models (MaxEnt) for the study species show Panicoideae NADP-Me species (Figure 2a) to have the highest H.S. in a narrow belt along the eastern portion of southern Africa, coinciding with areas of relatively high mean annual precipitation (Figure 2d). Panicoideae NAD-Me species (Figure 2b) show high H.S. throughout most of southern Africa, with the exception of the high rainfall areas including and north of Angola and Zambia. Aristidoideae NADP-Me species (Figure 2c) show the highest H.S. in the relatively drier regions of South Africa, Namibia and Tanzania.

The geographical differences in species H.S. were strongly related to mean annual precipitation (Figure 3a). Peak H.S. occurs at notably lower mean annual precipitation for both Panicoideae NAD-Me and Aristidoideae NADP-Me species relative to that of the Panicoideae NADP-Me species ($\chi^2 = -9.09$, $p < 0.001$). Although both the Panicoideae NAD-Me and Aristidoideae NADP-Me species display peak occurrence at similar mean annual precipitation, the Panicoideae NAD-Me species maintain relatively high H.S. even at higher precipitation levels, while the Aristidoideae NADP-Me species are constrained to areas of lower precipitation. In order to confirm that these patterns hold true across the groups, a broader scale modelling effort was conducted using multiple Panicoideae and Aristidoideae species which occur in southern Africa (Figure 3b). Similar to the study species-only models, peak H.S. is at lower mean annual precipitation in the Aristidoideae species than in the Panicoideae species ($\chi^2 = -42.42$, $p < 0.0001$). Figure S1 provides details of the contribution of all 19 environmental drivers for the models.

3.2 | Drought susceptibility constrained by phylogeny and photosynthetic subtype

Figures 4 and 5 show only results for plants exposed to drought to display drought responses over time and drought recovery. Watered (control) comparisons are presented in Figure S2 and remained relatively constant over time when compared to the drought treatment, differing significantly from drought plants despite some variability within the control treatment (Table S4). Photosynthetic impairment as drought progressed and recovery from drought differed between both photosynthetic subtypes and phylogenetic groups. Net assimilation rates measured at growth C_a of 400 ppm were maintained at slightly higher rates as drought progressed in the Aristidoideae NADP-Me relative to both Panicoideae groups (Figure 4a; $F_{2,204} = 0.24$, $p = 0.79$) and displayed significantly more rapid recovery postdrought (Figure 4a; $F_{2,137} = 9.32$, $p < 0.05$). This appears to be partly due to the maintenance of relatively high G_{st} in the Aristidoideae NADP-Me species during both the dry-down (Figure 5b; $F_{2,204} = 0.59$, $p = 0.58$) and recovery periods (Figure 5b; $F_{2,137} = 13.06$, $p < 0.01$). The Aristidoideae NADP-Me and Panicoideae NADP-Me showed small, but nonsignificant increases in C_i at peak drought relative to the Panicoideae NAD-Me species (Figure 4c; $F_{2,6} = 0.73$, $p = 0.52$), indicating possible metabolic impairment for the latter. Although all Panicoideae species were more susceptible to drought than the Aristidoideae species, the Panicoideae NAD-Me species were also

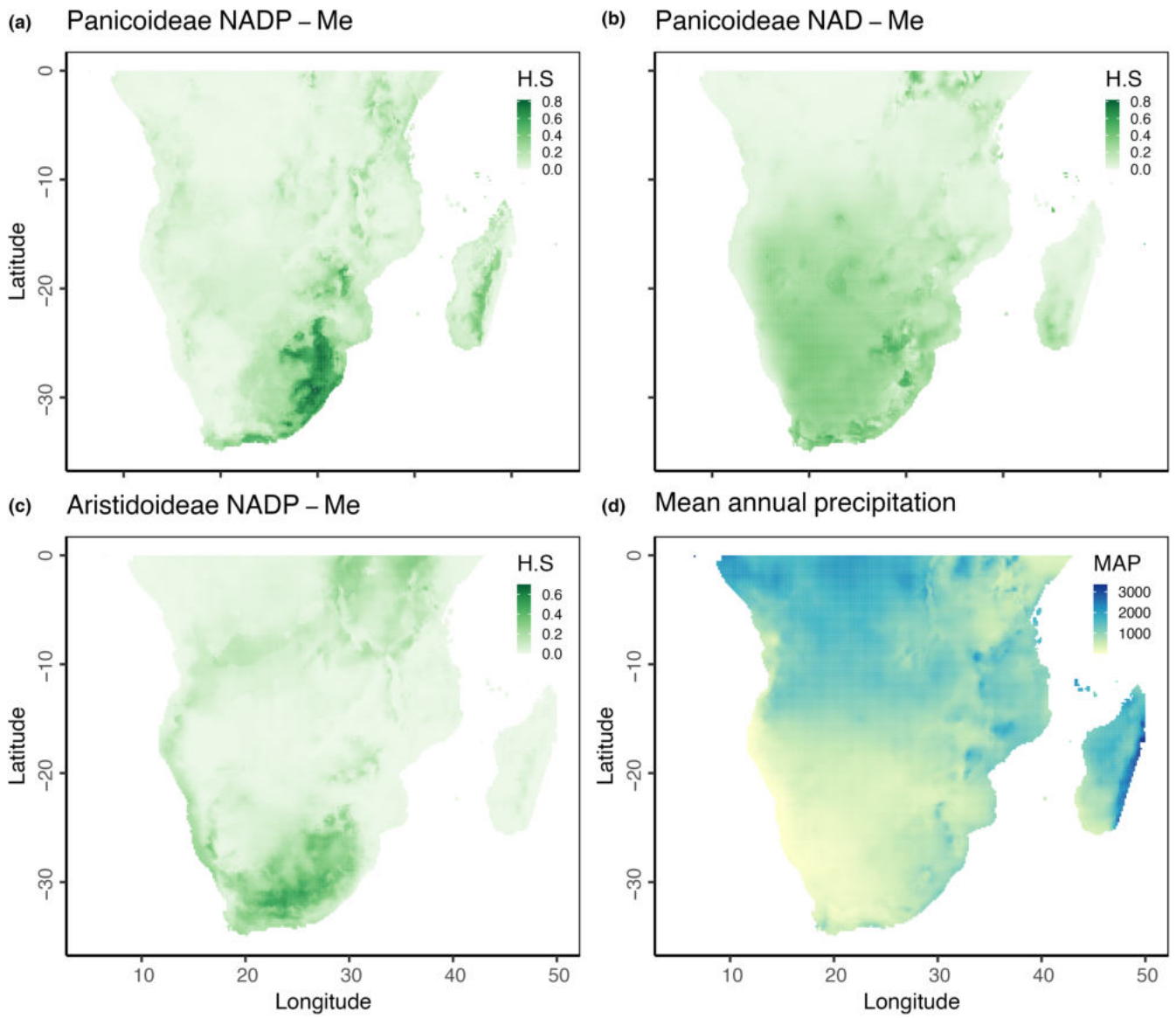

FIGURE 2 Predicted habitat suitability (H.S.) in southern Africa using MaxEnt for three species of NADP-Me Panicoideae C_4 grasses (*Heteropogon contortus*, *Alloteropsis semialata* and *Tristachya leucothrix*) (a), two species of NAD-Me Panicoideae C_4 grasses (*Panicum coloratum* and *P. stapfianum*) (b), three species of Aristidoideae C_4 grasses (*Aristida congesta*, *A. diffusa* and *A. junciformis*) (c), and mean annual precipitation (d) (Worldclim; Fick & Hijmans, 2017).

able to recover their photosynthetic rates more rapidly than their NADP-Me counterparts.

Both the Aristidoideae NADP-Me and Panicoideae NAD-Me species maintained higher RLWC during the dry-down period (Figure 4d; $F_{2,178}=13.31$, $p<0.01$) than the Panicoideae NADP-Me species. Leaf Ψ was maintained at less negative values in the Aristidoideae NADP-Me and Panicoideae NAD-Me groups relative to the Panicoideae NADP-Me during the dry-down (Figure 4e; $F_{2,133}=3.68$, $p<0.05$) but did not differ between groups during the recovery period (Figure 4e; $F_{2,62}=0.19$, $p=0.66$). The mechanisms for this maintenance of RLWC and Leaf Ψ differ between the two groups, with the Aristidoideae NADP-Me species achieving this at least partly through osmotic adjustment during the dry-down (Figure 4f; $F_{2,102}=3.79$, $p<0.05$) and the Panicoideae NAD-Me species through greater reduction in G_{st} (Figure 4b) during periods of severe drought. The Panicoideae NADP-Me species displayed low G_{st} in response to drought, but also exhibited signs of metabolic impairment. Sharp decreases in values of ETR/*A* at peak drought demonstrate greater metabolic impairment in the Panicoideae NADP-Me species at the most severe point of the drought, although this response is not significant over the entire experiment (Figure 5c; $F_{2,153}=0.10$, $p=0.90$ during dry-down and $F_{2,78}=0.01$, $p=0.99$ during recovery). Φ PSII/*A*, representative of light reaction activity relative to CO_2 assimilation, shows a similar response (Figure 5a; $F_{2,204}=0.62$, $p=0.57$ during dry-down and $F_{2,137}=0.63$, $p=0.57$ during recovery). Fv′Fm′ was significantly lower in the Panicoideae NAD-Me species relative to both NADP-Me groups during the dry-down (Figure 5b; $F_{2,204}=5.77$, $p<0.01$), but recovered significantly faster in the Aristidoideae

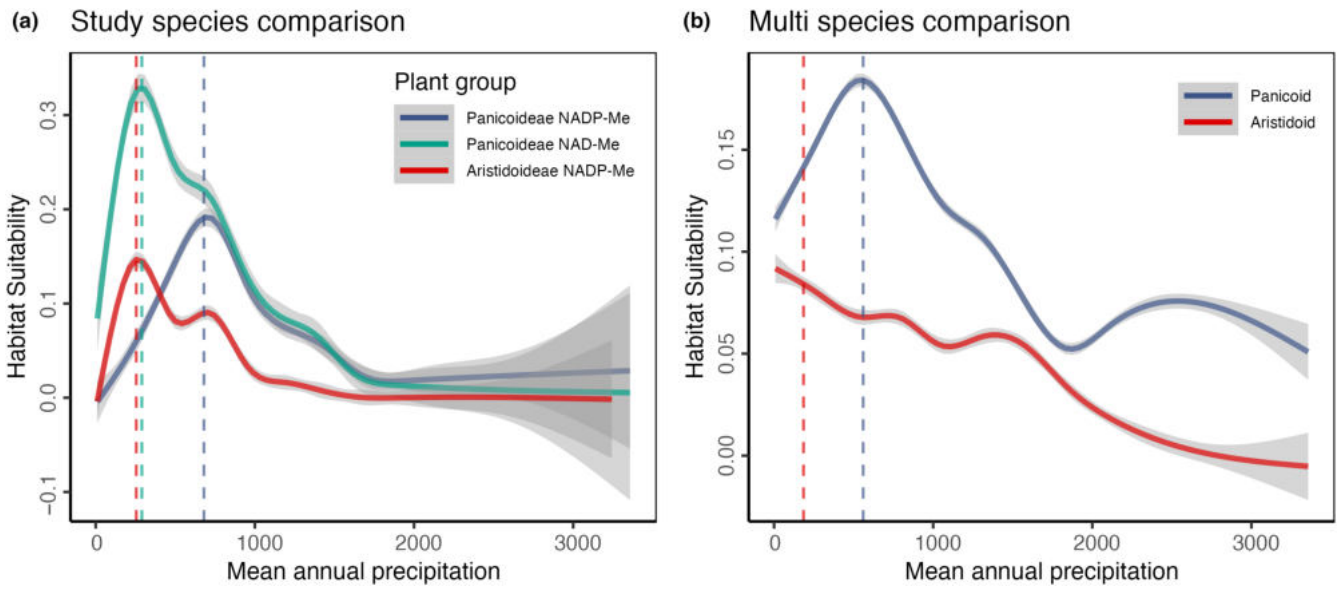

FIGURE 3 Predicted habitat suitability in southern Africa using MaxEnt for the species used in this study: three species of NADP-Me Panicoideae C_4 grasses (*Heteropogon contortus*, *Alloteropsis semialata* and *Tristachya leucothrix*), two species of NAD-Me Panicoideae C_4 grasses (*Panicum coloratum* and *P. stapfianum*), and three species of Aristidoideae C_4 grasses (*Aristida congesta*, *A. diffusa* and *A. junciformis*) (a), and for multiple species of Panicoideae and Aristidoideae C_4 grasses (b) (see Table S1 for a list of species). Showing mean ± 95% CI.

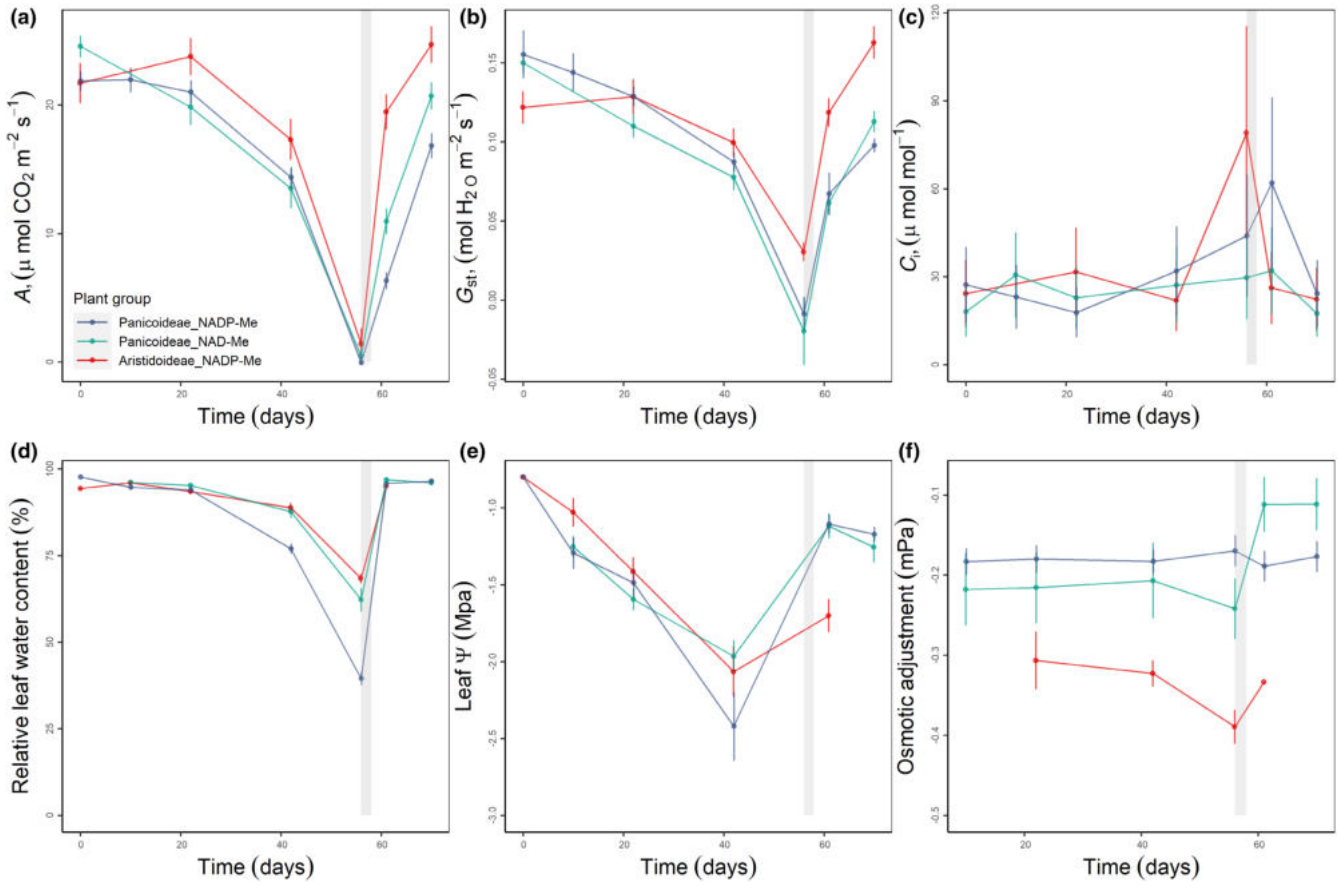

FIGURE 4 Net assimilation rate (*A*) (a), stomatal conductance (G_{st}) (b), intercellular CO_2 (C_i) (c), relative leaf water content (RLWC) (d), leaf water potential (Leaf Ψ) (e) and osmotic adjustment (f) for NADP-Me Panicoideae C_4 grasses (*Heteropogon contortus*, *Alloteropsis semialata* and *Tristachya leucothrix*), NAD-Me Panicoideae C_4 grasses (*Panicum coloratum* and *P. stapfianum*) and Aristidoideae NAPD-Me C_4 grasses (*Aristida congesta*, *A. diffusa* and *A. junciformis*). Grey bar shows the time where pots were rewatered. Showing mean ± SE.

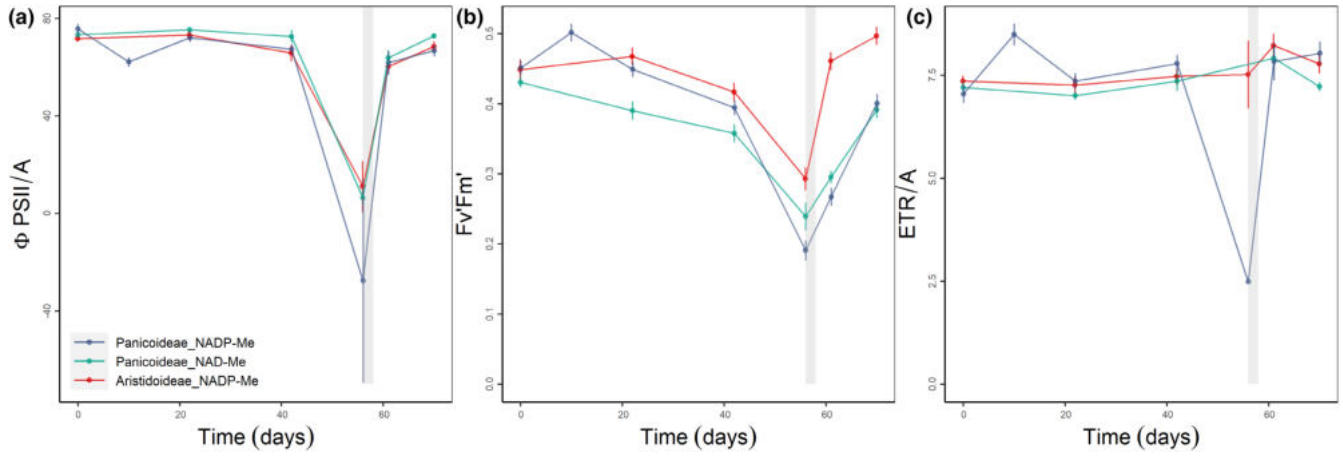

FIGURE 5 A/ΦPSII (a), Fv′Fm′ (b) and ETR/*A* (c) for NADP-Me Panicoideae C_4 grasses (*Heteropogon contortus*, *Alloteropsis semialata* and *Tristachya leucothrix*), NAD-Me Panicoideae C_4 grasses (*Panicum coloratum* and *P. stapfianum*) and Aristidoideae NAPD-Me C_4 grasses (*Aristida congesta*, *A. diffusa* and *A. junciformis*). Grey bar shows the time where pots were rewatered. Showing mean ± SE.

NADP-Me species relative to both Panicoideae groups (Figure 5b; $F_{2,137} = 1.48$, $p < 0.01$). Figure S5 shows analysis of the relatedness of this suite of physiological parameters.

4 | DISCUSSION

Using selected southern African C_4 grass species as a model for subtype and phylogenetic differences in C_4 grass drought tolerances, we show both photosynthetic subtype and phylogeny to play a role in drought susceptibility and resultant species distribution patterns in relation to rainfall. This was done by comparing (1) plants with different photosynthetic subtypes from the same lineage (Panicoideae) and (2) plants sharing the same biochemistry (NADP-Me), but from different lineages (Panicoideae and Aristidoideae). Owing to the natural distributions of C_4 grasses within South Africa and their association to rainfall gradients, it was hypothesized that Panicoideae NAD-Me and Aristidoideae NADP-Me species would exhibit greater drought tolerance over Panicoideae NADP-Me species. We confirm here that species distributions in relation to water availability are as expected based on the literature and that physiological differences between the three groups can help explain distribution patterns. We provide novel insight into the mechanisms by which species are more or less susceptible to drought.

Species distribution modelling including all possible species from the groups present in southern Africa found the Panicoideae group to be more dependent on rainfall than the Aristidoideae group, for which the H.S. peaks at significantly lower MAP than for the Panicoideae. This pattern holds for our study species, with the Panicoideae NADP-Me species displaying peak H.S. at significantly higher MAP than both the Panicoideae NAD-Me and Aristidoideae NADP-Me species. This exhibits the interactive effects of photosynthetic subtype (as shown by Taub, 2000) and phylogeny (as shown by Visser et al., 2012) in C_4 grass distributions.

The differences seen in species distributions were reflected by plant physiological responses to drought. The Panicoideae NADP-Me species showed the highest drought susceptibility with extreme decreases in RLWC and photosynthetic rates as drought progressed and the slowest rates of recovery postdrought. The Panicoideae NAD-Me species, on the other hand, were able to maintain leaf water content at significantly higher levels than NADP-Me Panicoids and were able to recover their photosynthetic rates more rapidly postdrought. The Aristidoideae NADP-Me species showed the lowest drought susceptibility, maintaining relatively high leaf water content, maintaining photosynthetic rates for longer into the drought period, and showing significantly faster recovery postdrought than both Panicoideae groups.

The notable drought susceptibility in the Panicoideae NADP-Me species appears to be due to greater metabolic impairment relative to the other groups. Metabolic limitations were likely responsible as the C_i of the Panicoideae NADP-Me at day 61 (3 days post rewatering) was 192% higher than the C_i of the NAD-Me subtype, while G_{st} values were not different. This is an indication that photosynthetic processes were not stomatally limited but rather metabolically limited and the plants were unable to utilize the available C_i. This is supported by ETR/*A* ratios which progressively increased for Panicoideae NADP-Me species with drought, indicating an increase in the energetic cost per CO_2 fixed (Ripley et al., 2007). Panicoideae NADP-Me responses presented here support the current literature which shows that metabolic limitation was a significant contributor to the decline in photosynthesis in droughted C_4 grasses (Da Silva & Arrabaca, 2004; Ghannoum et al., 2003; Lawlor, 2002; Ripley et al., 2007, 2010).

The mechanisms by which the Panicoideae NAD-Me and Aristidoideae NADP-Me species were able to maintain higher RLWC than the Panicoideae NADP-Me species differed between the two groups. In the case of the Panicoideae NAD-Me species, maintenance of plant water status was through greater reduction in G_{st} preventing water loss through transpiration. The data presented

here cannot fully elucidate the cause of this difference between the Panicoideae NADP-Me and NAD-Me, but we propose that the difference may be linked to the additional metabolic costs of the NADP-Me process (Furbank, 2011; Kanai & Edwards, 1999). While the NAD-Me subtype can derive bundle sheath NADPH and ATP via their own light reactions, the NADP-Me subtype involves additional complexity in the reduction of PGA (phosphoglycerate).

On the other hand, the Aristidoideae NADP-Me species were able to maintain plant water status through greater osmotic adjustment. It is well documented that plants utilize osmotic adjustment as a mechanism to maintain leaf turgor potential by lowering the Leaf Ψ in response to drought, allowing cells to maintain important metabolic processes (Baruch & Fernández, 1993; Girma & Krieg, 1992; Jones & Turner, 1978). Increased osmotic adjustment meant that plants were able to maintain higher G_{st} and maintain photosynthetic rates even as water became limiting. The Aristidoideae NADP-Me species were thus able to prevent severe metabolic limitation as drought progressed. Previous studies have shown a similar association of osmotic adjustment to more drought-tolerant species (Girma & Krieg, 1992; Jones & Turner, 1978; Kusaka et al., 2005).

The phylogenetic differences seen here can be partly described using the characteristic differences between anisohydric and isohydric plants. The Aristidoideae NADP-Me species showed properties associated with anisohydric plants, which keep their stomata open, irrespective of Leaf Ψ, maintain higher photosynthetic rates during mild to moderate drought conditions, and are generally classified as drought tolerant (McDowell et al., 2008). Both groups of Panicoideae species tended to resemble the behaviour of isohydric plants, which operate at lower G_{st} during drought to maintain constant Leaf Ψ, resulting in lower photosynthetic rates under drought situations (McDowell et al., 2008). Isohydric regulation is seen as a mechanism to avoid hydraulic failure (i.e. cavitation), whereas anisohydric plants are vulnerable to hydraulic failure due to small hydraulic safety margins during drought episodes (McDowell et al., 2008). However, the Aristidoideae species shown here maintained high RLWC during drought through osmotic adjustment, possibly mitigating the effects of cavitation. It has been shown that under severe drought conditions, isohydric and anisohydric grasses showed little difference in their photosynthetic responses (Alvarez et al., 2007), and results here showed that the Panicoideae and Aristidoideae species all responded similarly at severe drought (day 56; ~3.5% SWC) regardless of photosynthetic subtype. The differences we show are therefore related to how rapidly photosynthesis declines with exposure to drought and the rate of recovery postdrought, rather than the maximum extent of photosynthetic decline.

We show here that drought susceptibility differs between C_4 photosynthetic subtypes, but that phylogeny plays an equal to greater role. From an ecological perspective, this adds valuable insight in the face of the predicted increases in aridity for southern Africa (Engelbrecht et al., 2015). Results presented here suggest that increases in the extent and severity of drought may allow drought-tolerant species such as the Aristidoideae to expand their range and possibly outcompete other species such as the Panicoideae, particularly the NADP-Me subtype. Furthermore, mesic grasslands that are dominated by Panicoideae species may be vulnerable to changes in functional type compositions.

AUTHOR CONTRIBUTIONS

Sarah L. Raubenheimer, Brad S. Ripley and Nic Venter conceived the ideas and designed the methodology; Nic Venter and Brad S. Ripley collected the data; Sarah L. Raubenheimer and Nic Venter analysed the data; Sarah L. Raubenheimer led the writing of the manuscript. All authors contributed critically to the drafts and gave final approval for publication.

ACKNOWLEDGEMENTS

Research support was provided by Rhodes University. We thank Dr Riaan Strauss and Mr William Ntleki for assistance with experimental and laboratory work.

CONFLICT OF INTEREST STATEMENT

The authors do not have any conflict of interest to state.

DATA AVAILABILITY STATEMENT

Data available from the Dryad Digital Repository: https://doi.org/10.5061/dryad.tdz08kq46 (Raubenheimer, 2023).

ORCID

Sarah L. Raubenheimer https://orcid.org/0000-0001-7219-4631
Nic Venter https://orcid.org/0000-0003-3509-2331
Brad S. Ripley https://orcid.org/0000-0002-4546-2618

REFERENCES

Alvarez, E., Scheiber, S. M., Beeson, R. C., & Sandrock, D. R. (2007). Drought tolerance responses of purple lovegrass and 'adagio' maiden grass. *HortScience*, *42*(7), 1695–1699.

Baker, N. R. (2008). Chlorophyll fluorescence: A probe of photosynthesis in vivo. *Annual Review of Plant Biology*, *59*, 89–113.

Baruch, Z., & Fernández, D. S. (1993). Water relations of native and introduced C_4 grasses in a neotropical savanna. *Oecologia*, *96*(2), 179–185.

Cabido, M., Pons, E., Cantero, J. J., Lewis, J. P., & Anton, A. (2008). Photosynthetic pathway variation among C_4 grasses along a precipitation gradient in Argentina. *Journal of Biogeography*, *35*(1), 131–140.

Carmo-Silva, A. E., Francisco, A., Powers, S. J., Keys, A. J., Ascensão, L., Parry, M. A., & Arrabaça, M. C. (2009). Grasses of different C_4 subtypes reveal leaf traits related to drought tolerance in their natural habitats: Changes in structure, water potential, and amino acid content. *American Journal of Botany*, *96*(7), 1222–1235.

Da Silva, J. M., & Arrabaca, M. C. (2004). Photosynthesis in the water-stressed C_4 grass *Setaria sphacelata* is mainly limited by stomata with both rapidly and slowly imposed water deficits. *Physiologia Plantarum*, *121*(3), 409–420.

Edwards, E. J., & Still, C. J. (2008). Climate, phylogeny and the ecological distribution of C_4 grasses. *Ecology Letters*, *11*(3), 266–276.

Elith, J., Phillips, S. J., Hastie, T., Dudík, M., Chee, Y. E., & Yates, C. J. (2011). A statistical explanation of MaxEnt for ecologists. *Diversity and Distributions*, *17*(1), 43–57. https://doi.org/10.1111/j.1472-4642.2010.00725.x

Ellis, R. P., Vogel, J. C., & Fuls, A. (1980). Photosynthetic pathways and the geographical distribution of grasses in South West Africa/Namibia. *South African Journal of Science*, *76*(7), 307–314.

Engelbrecht, F., Adegoke, J., Bopape, M. J., Naidoo, M., Garland, R., Thatcher, M., McGregor, J., Katzfey, J., Werner, M., Ichoku, C., & Gatebe, C. (2015). Projections of rapidly rising surface temperatures over Africa under low mitigation. *Environmental Research Letters*, *10*(8), 085004.

Fick, S. E., & Hijmans, R. J. (2017). WorldClim 2: New 1-km spatial resolution climate surfaces for global land areas. *International Journal of Climatology*, *37*(12), 4302–4315.

Furbank, R. T. (2011). Evolution of the C_4 photosynthetic mechanism: Are there really three C_4 acid decarboxylation types? *Journal of Experimental Botany*, *62*(9), 3103–3108.

Gbif.org. (2021). *Global Biodiversity Information Facility (GBIF) occurrence download*.

Ghannoum, O., Conroy, J. P., Driscoll, S. P., Paul, M. J., Foyer, C. H., & Lawlor, D. W. (2003). Nonstomatal limitations are responsible for drought-induced photosynthetic inhibition in four C_4 grasses. *New Phytologist*, *159*(3), 599–608.

Ghannoum, O., Von Caemmerer, S., & Conroy, J. P. (2002). The effect of drought on plant water use efficiency of nine NAD–ME and nine NADP–ME Australian C_4 grasses. *Functional Plant Biology*, *29*(11), 1337–1348.

Girma, F. S., & Krieg, D. R. (1992). Osmotic adjustment in sorghum: I. Mechanisms of diurnal osmotic potential changes. *Plant Physiology*, *99*(2), 577–582.

Hastie, T. (2020). *gam: Generalized additive models (version R package Version 1.20). CRAN*.

Hattersley, P. W., & Watson, L. (1992). Diversification of photosynthesis. *Grass Evolution and Domestication*, *38*, 116.

Jones, M. M., & Turner, N. C. (1978). Osmotic adjustment in leaves of sorghum in response to water deficits. *Plant Physiology*, *61*(1), 122–126.

Kanai, R., & Edwards, G. E. (1999). The biochemistry of C_4 photosynthesis. *C4 Plant Biology*, *49*, 87.

Kusaka, M., Ohta, M., & Fujimura, T. (2005). Contribution of inorganic components to osmotic adjustment and leaf folding for drought tolerance in pearl millet. *Physiologia Plantarum*, *125*(4), 474–489.

Lawlor, D. W. (2002). Limitation to photosynthesis in water-stressed leaves: Stomata vs. metabolism and the role of ATP. *Annals of Botany*, *89*(7), 871–885.

Liu, H., & Osborne, C. P. (2015). Water relations traits of C_4 grasses depend on phylogenetic lineage, photosynthetic pathway, and habitat water availability. *Journal of Experimental Botany*, *66*(3), 761–773.

Long, S. P., & Bernacchi, C. J. (2003). Gas exchange measurements, what can they tell us about the underlying limitations to photosynthesis? Procedures and sources of error. *Journal of Experimental Botany*, *54*(392), 2393–2401.

McDowell, N., Pockman, W. T., Allen, C. D., Breshears, D. D., Cobb, N., Kolb, T., Plaut, J., Sperry, J., West, A., Williams, D. G., & Yepez, E. A. (2008). Mechanisms of plant survival and mortality during drought: Why do some plants survive while others succumb to drought? *New Phytologist*, *178*(4), 719–739.

Phillips, S. J., Dudík, M., Elith, J., Graham, C. H., Lehmann, A., Leathwick, J., & Ferrier, S. (2009). Sample selection bias and presence-only distribution models: Implications for background and pseudo-absence data. *Ecological Applications*, *19*(1), 181–197. https://doi.org/10.1890/07-2153.1

Pinheiro, J., Bates, D., DebRoy, S., Sarkar, D., & Team, R. C. (2007). *Linear and nonlinear mixed effects models*. R package version, 3(57), 1–89.

Pinto, H., Powell, J. R., Sharwood, R. E., Tissue, D. T., & Ghannoum, O. (2016). Variations in nitrogen use efficiency reflect the biochemical subtype while variations in water use efficiency reflect the evolutionary lineage of C_4 grasses at inter-glacial CO_2. *Plant, Cell & Environment*, *39*(3), 514–526.

R Core Team. (2020). *R: A language and environment for statistical computing*. R Foundation for Statistical Computing. https://www.R-project.org/

Raubenheimer, S. (2023). Drought susceptibility of southern African C_4 grasses: Phylogenetically and photosynthetically determined? *Dryad*, *Dataset*. https://doi.org/10.5061/dryad.tdz08kq46

Ripley, B., Frole, K., & Gilbert, M. (2010). Differences in drought sensitivities and photosynthetic limitations between co-occurring C_3 and C_4 (NADP-ME) Panicoid grasses. *Annals of Botany*, *105*(3), 493–503.

Ripley, B. S., Gilbert, M. E., Ibrahim, D. G., & Osborne, C. P. (2007). Drought constraints on C_4 photosynthesis: Stomatal and metabolic limitations in C_3 and C_4 subspecies *of Alloteropsis semialata*. *Journal of Experimental Botany*, *58*(6), 1351–1363.

Sage, R. F. (2004). The evolution of C_4 photosynthesis. *New Phytologist*, *161*(2), 341–370.

Sage, R. F., & Monson, R. K. (1998). *C_4 plant biology*. Elsevier.

Schulte, P. J., & Hinckley, T. M. (1985). A comparison of pressure-volume curve data analysis techniques. *Journal of Experimental Botany*, *36*(10), 1590–1602.

Smith, S. A., & Donoghue, M. J. (2008). Rates of molecular evolution are linked to life history in flowering plants. *Science*, *322*(5898), 86–89.

Taub, D. R. (2000). Climate and the US distribution of C_4 grass subfamilies and decarboxylation variants of C_4 photosynthesis. *American Journal of Botany*, *87*(8), 1211–1215.

Taylor, S. H., Hulme, S. P., Rees, M., Ripley, B. S., Ian Woodward, F., & Osborne, C. P. (2010). Ecophysiological traits in C_3 and C_4 grasses: A phylogenetically controlled screening experiment. *New Phytologist*, *185*(3), 780–791. https://doi.org/10.1111/j.1469-8137.2009.03102.x

Tieszen, L. L., Senyimba, M. M., Imbamba, S. K., & Troughton, J. H. (1979). The distribution of C_3 and C_4 grasses and carbon isotope discrimination along an altitudinal and moisture gradient in Kenya. *Oecologia*, *37*(3), 337–350.

Visser, V., Woodward, F. I., Freckleton, R. P., & Osborne, C. P. (2012). Environmental factors determining the phylogenetic structure of C_4 grass communities. *Journal of Biogeography*, *39*(2), 232–246.

Vogel, J. C., Fuls, A., & Danin, A. (1986). Geographical and environmental distribution of C_3 and C_4 grasses in the Sinai, Negev, and Judean deserts. *Oecologia*, *70*(2), 258–265.

Von Caemmerer, S. V., & Farquhar, G. D. (1981). Some relationships between the biochemistry of photosynthesis and the gas exchange of leaves. *Planta*, *153*(4), 376–387.

Wigley-Coetsee, C., & Staver, A. C. (2020). Grass community responses to drought in an African savanna. *African Journal of Range & Forage Science*, *37*(1), 43–52.

SUPPORTING INFORMATION

Additional supporting information can be found online in the Supporting Information section at the end of this article.

Figure S1. Contribution of environmental predictor variables to MaxEnt habitat suitability (H.S) for Aristidoideae and Panicoideae species.

Figure S2. Net assimilation rate (*A*) (A), stomatal conductance (G_{st}) (B), intercellular CO_2 concentration (C_i) (C), relative leaf water content (D), leaf water potential (Leaf Ψ) (E), and Φ PSII (F) for well-watered (i.e., control) NADP-Me Panicoideae C_4 grasses (*Heteropogon contortus*, *Alloteropsis semialata* and *Tristachya leucothrix*), NAD-Me Panicoideae C_4 grasses(*Panicum coloratum* and *P. stapfianum*), and Aristidoideae NAPD-Me C_4 grasses (*Aristida congesta*, *A. diffusa* and *A. junciformis*)

Figure S3. Ψ_{Leaf} against relative leaf water content.

Figure S4. Pressure volume (PV) curves for watered NADP-Me Panicoideae C_4 grasses (*Heteropogon contortus*, *Alloteropsis semialata* and *Tristachya leucothrix*), NAD-Me Panicoideae C_4 grasses (*Panicum coloratum* and *P. stapfianum*), and Aristidoideae NAPD-Me C_4 grasses (*Aristida congesta*, *A. diffusa* and *A. junciformis*).

Figure S5. Principal component analysis (PCA) displaying the relatedness of the suite of physiological responses measurement, comparing between three groups of C_4 grasses at peak drought (day 56). This shows NADP-Me Panicoideae C_4 grasses (*Heteropogon contortus*, *Alloteropsis semialata* and *Tristachya leucothrix*), NAD-Me Panicoideae C_4 grasses (*Panicum coloratum* and *P. stapfianum*), and Aristidoideae NAPD-Me C_4 grasses (*Aristida congesta*, *A. diffusa* and *A. junciformis*). Variables considered are water use efficiency (WUE), carbon assimilation rate (*A*), electron transport rate (ETR), quantum yield of electron transfer at PSII (ΦPSII), fluorescence/maximum fluorescence (Fv′Fm′), stomatal conductance (G_{st}), and relative leaf water content (RLWC). Longer vectors (variables) have a larger influence on the PC ordination, vectors that form a shallow angle show a positive correlation to one another, vectors at 90° are not well correlated and vectors at 180° infer a negative correlation. PC1 explains 80% of the variance and PC2 explains 17% of the variance.

Table S1. List of species modeled with MaxEnt providing area under the curve (AUC) values for each model.

Table S2. Description of environmental layers used in MaxEnt models.

Table S3. Description of species used in the experimental manipulation.

Table S4. Statistical effects of drought treatment and plant group on the physiological parameters presented in Figure S2.

How to cite this article: Raubenheimer, S. L., Venter, N., & Ripley, B. S. (2023). Drought susceptibility of southern African C_4 grasses: Phylogenetically and photosynthetically determined? *Functional Ecology*, *37*, 2029–2039. https://doi.org/10.1111/1365-2435.14348